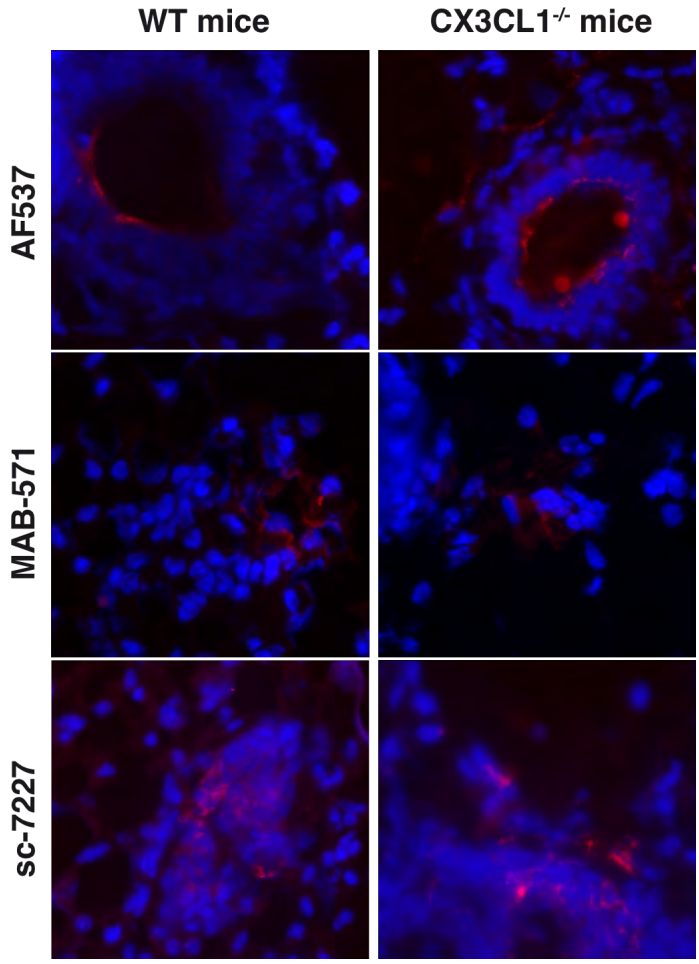

Supplementary Fig. S1. ***CX3CL1 staining in mammary glands of WT and CX3CL1$^{-/-}$ mice.*** Sections of mammary glands of 12-week-old nulliparous WT and CX3CL1$^{-/-}$ mice were stained with the anti-CX3CL1antibodies (red); nuclei were counterstained with DAPI. Images are representative of three independent experiments.

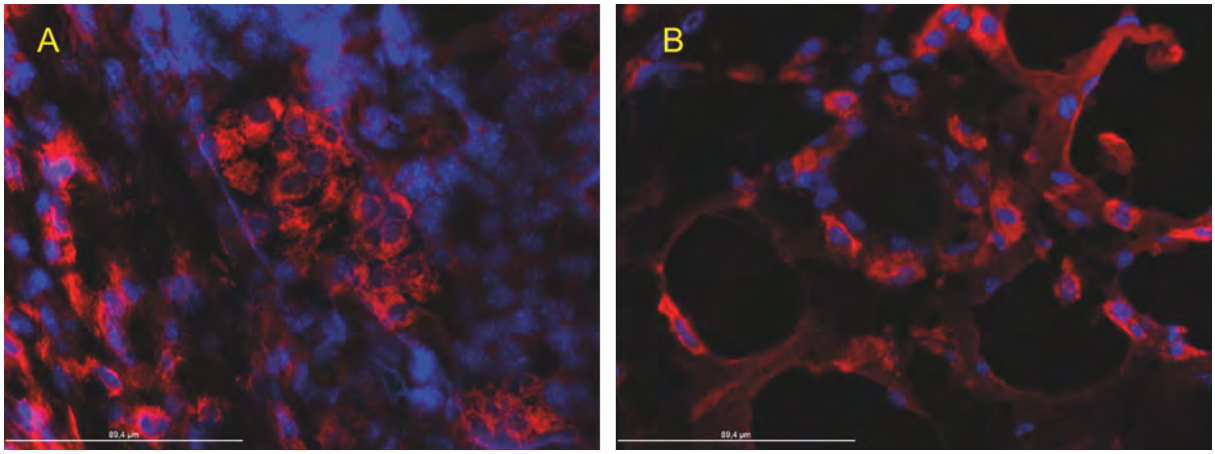

Supplementary Fig. S2. ***Staining of CX3CR1 in tumors and mammary glands of Tg-neu mice.*** Sections of breast tumors (A) and tumor-free mammary glands (C) of Tg-neu mice were stained with an in-house developed murine CX3CL1 fused to human Ig-Fc (red). Nuclei were counterstained with DAPI. Images are representative of two independent experiments. Bar = 90 μm

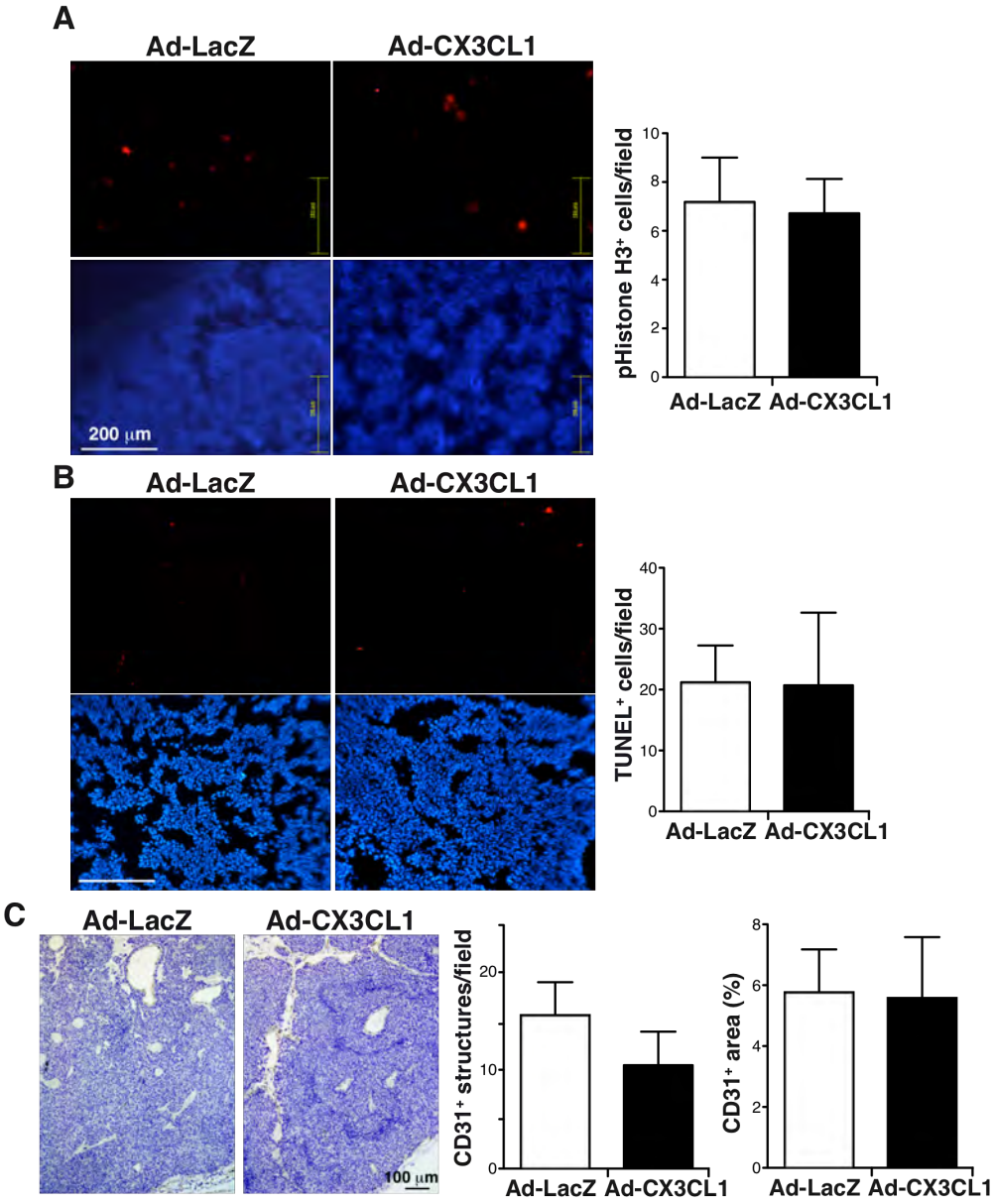

Supplementary Fig. S3. ***Effects of Ad-CX3CL1 or Ad-LacZ injection in tumor proliferation, apoptosis and angiogenesis.*** Representative images of sections from Ad-CX3CL1- and Ad-LacZ-injected tumors stained (red) for phospho Histone-H3 (*A*) and TUNEL (*B*) to determine the fraction of proliferating and apoptotic cells, respectively. Quantification of images is shown at the right (n = 4 mice/group, 8 fields per mouse). Bar, 200 μm. C, Ad-CX3CL1- and Ad-LacZ-injected tumors were stained for CD31 to visualize blood vessels (hematoxylin counterstaining). Quantification of the number of $CD31^+$ structures and the $CD31^+$-stained area is shown at the right (n = 4 mice/group, ≥ 10 fields per mouse)

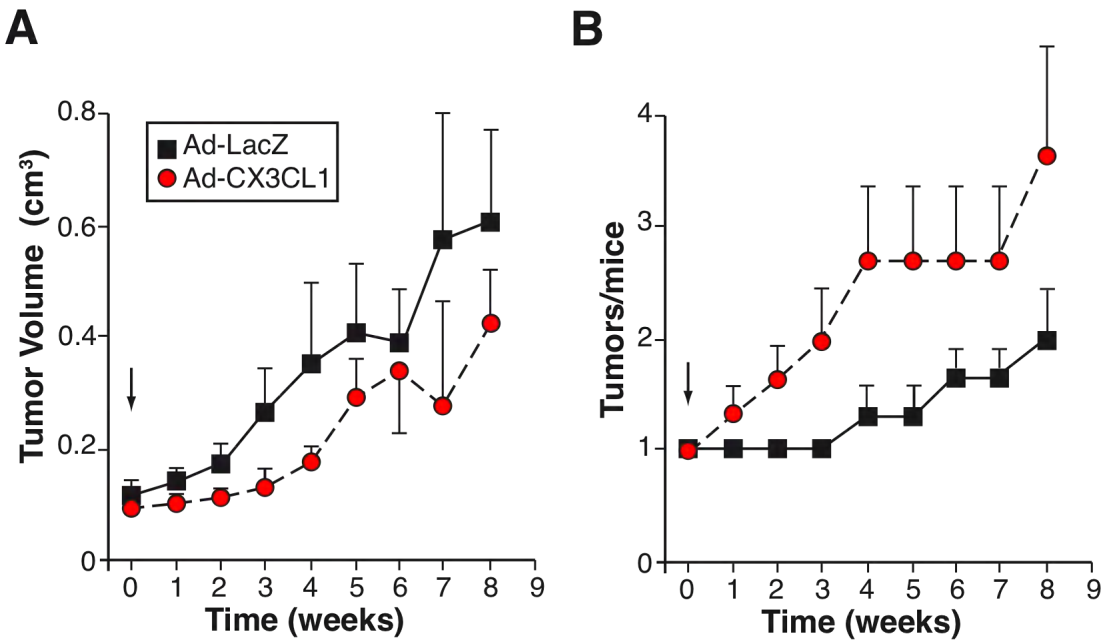

Supplementary Fig. S4. ***CX3CL1 overexpression increases breast carcinogenesis in Tg-neu mice.*** Tumor growth kinetics (A) and mean tumor number (B) in Tg-neu mice after a single intratumor injection (arrow) of Ad-CX3CL1 or Ad-LacZ virus. Data are mean ± SEM (n = 4 mice/group; two-way ANOVA with Bonferroni post-test).

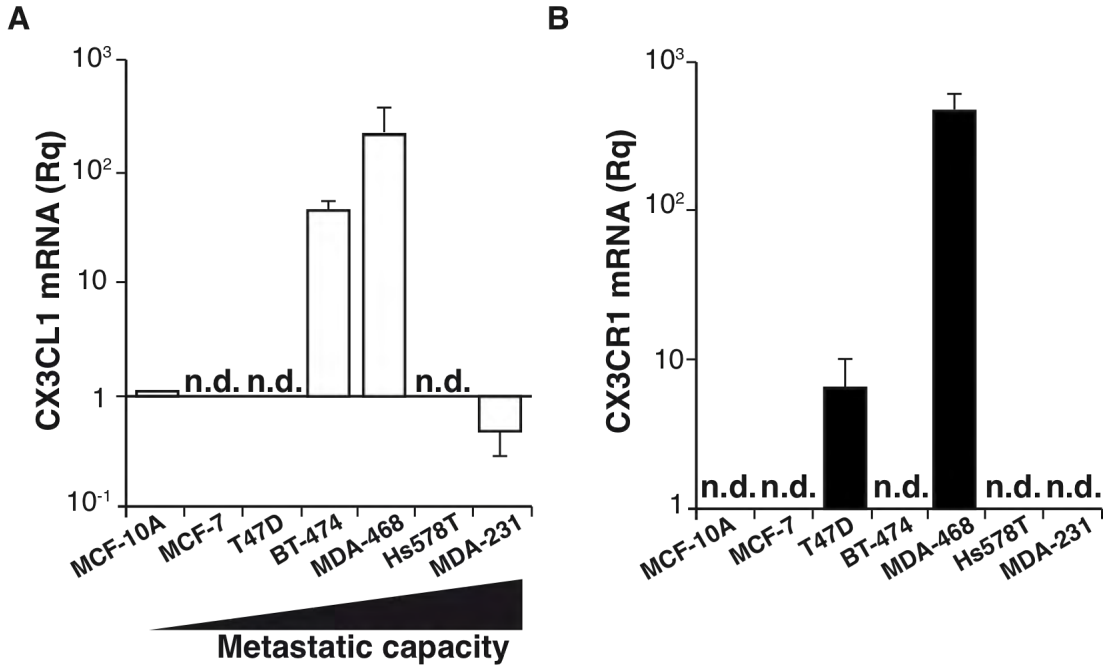

Supplementary Fig. S5. ***CX3CL1 or CX3CR1 mRNA expression in breast cancer cell lines with distinct metastatic potential.*** CX3CL1 (*A*) and CX3CR1 (*B*) mRNA levels in a panel of human breast cancer cell lines classified by their metastatic potential. The untransformed MCF-10A epithelial breast cell line was included as a control, and considered the reference value for calculation of relative quantity of CX3CL1 and CX3CR1 mRNA. Data are mean ± SEM of triplicates in one representative experiment of two; n.d., not detected.

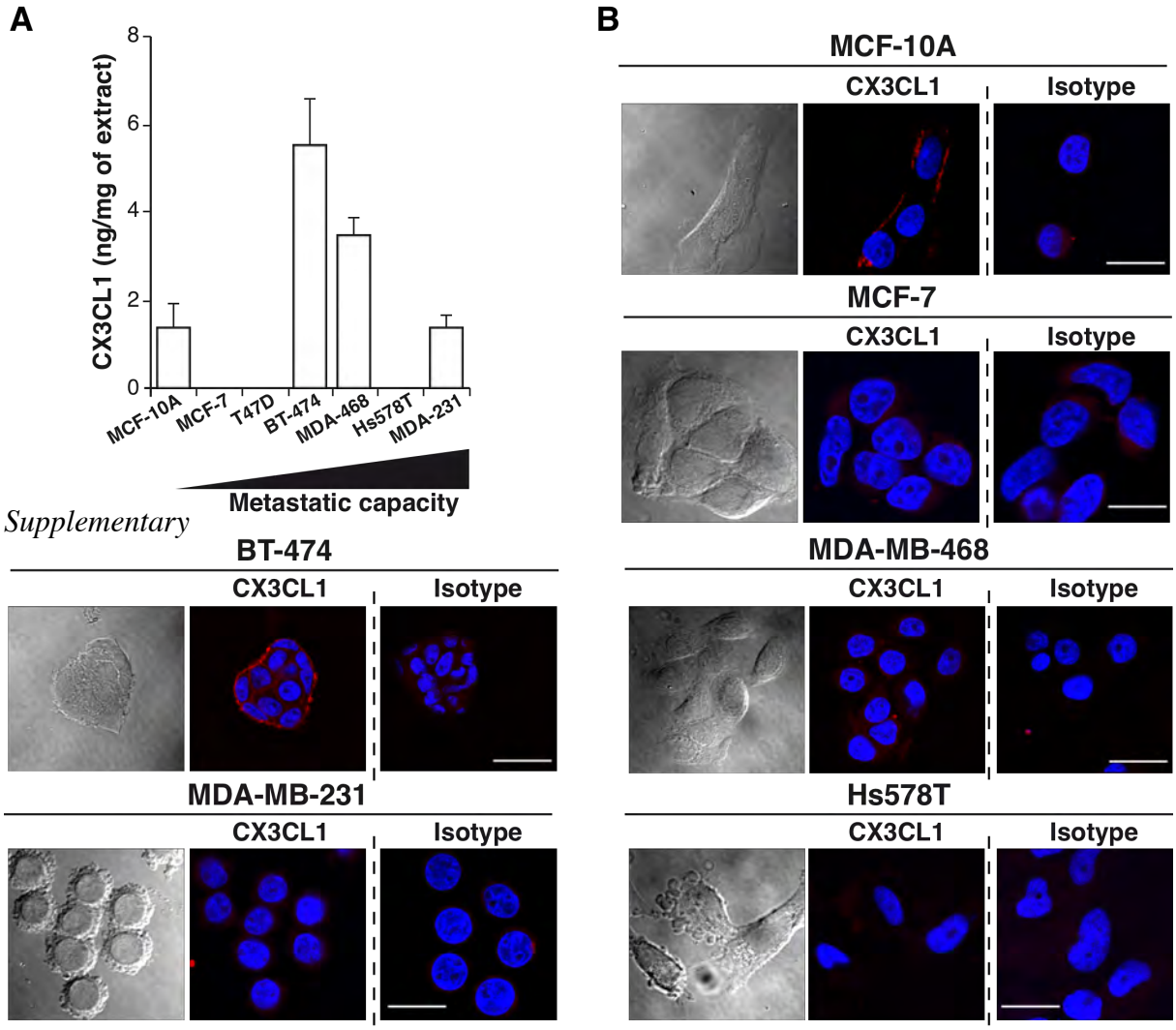

Supplementary

Fig. S6. ***CX3CL1 expression in a panel of breast cancer cell lines.*** A, CX3CL1 levels quantified by ELISA in a panel of human breast cancer cell lines. Data are mean ± SEM of triplicates in one representative experiment of three. B, Cells cultured on slides were stained with anti-human CX3CL1 antibody (AF 536, R&D systems); nuclei were DAPI-counterstained. All experiments were performed in parallel with an isotype-matched control antibody. Images are representative of at least 20 cells in each of three independent experiments. Bar = 15 μm, except for MCF-10A (bar = 25 μm) and BT-474 (bar = 30 μm).

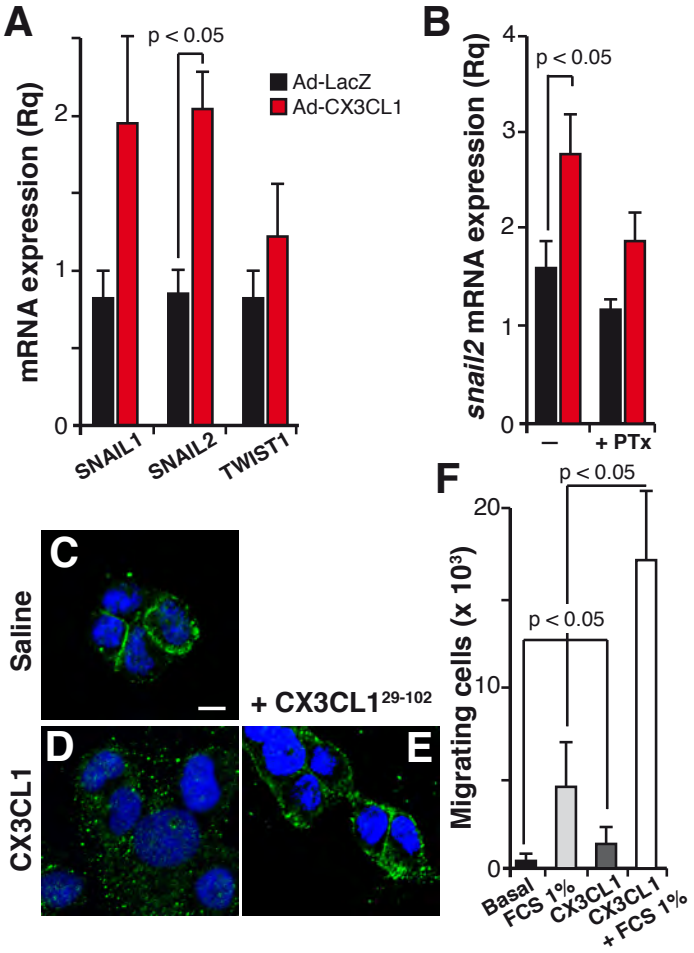

Supplementary Fig. S7. ***CX3CL1 induces EMT in breast cancer cells.*** A, Relative mRNA levels for the indicated genes in Ad-CX3CL1- and Ad-LacZ-infected T47D cells. B, Snail2 mRNA expression in Ad-CX3CL1 and and Ad-LacZ-infected T47D cells treated with vehicle (-) or pertussis toxin (+PTx). For A and B, data are expressed as a relative quantity using Ad-LacZ-infected cells as a reference (n = 3; one-tailed Student's t-test). C-E, Localization of E-cadherin (green) in T47D cells stimulated with saline (*C*), CX3CL1 (*D*) or CX3CL1 plus the antagonist CX3CL1$^{29\text{-}102}$ (*E*); nuclei were counterstained with DAPI. Cells are representative of 50 analyzed for each condition in two independent experiments; bar = 20 μm. F, T47D cell chemotaxis was assayed in transwell devices using the indicated doses of CX3CL1 in the absence (basal) or presence of 1% FCS. Data are mean ± SEM of triplicates (n = 2).

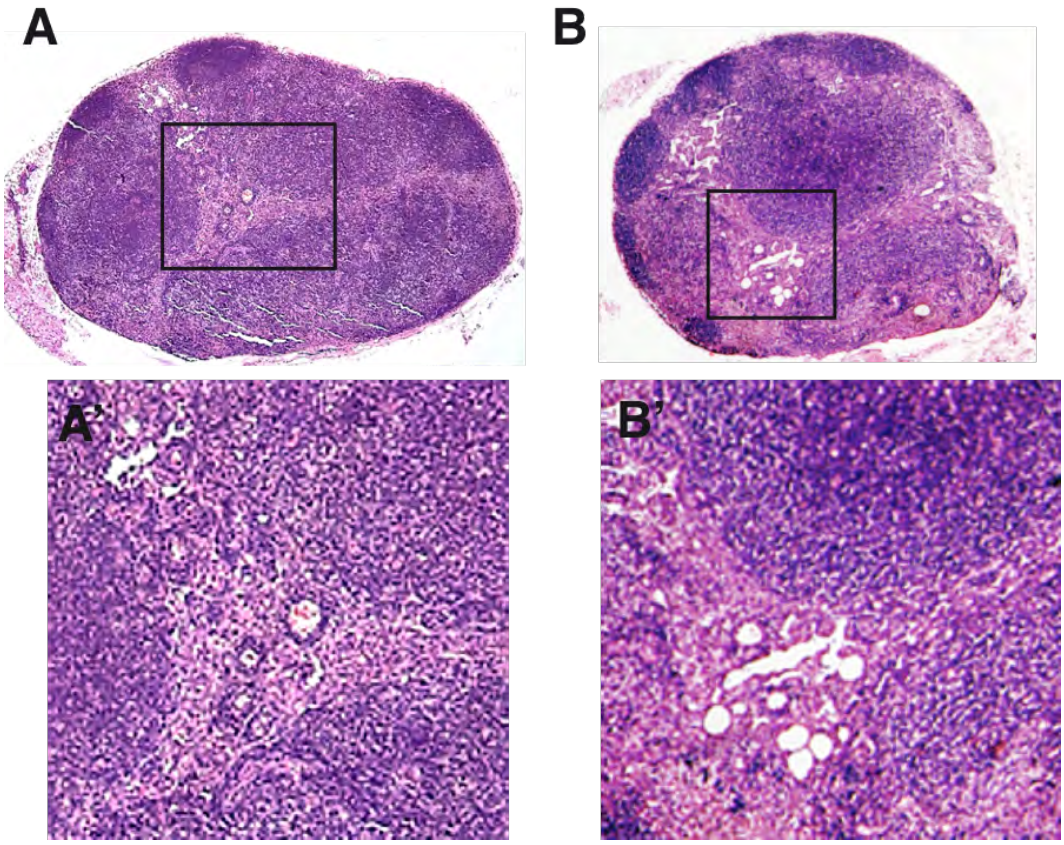

Supplementary Fig. S8. ***Lack of lymphoid metastases in Ad-CX3CL1-injected Tg-neu mice.*** A-B, Hematoxylin-eosin staining of LN adjacent to tumors from Ad-CX3CL1- (*A*) and Ad-LacZ-injected mice (*B*). Bottom panels (A', B') show digitally zoomed boxed areas.

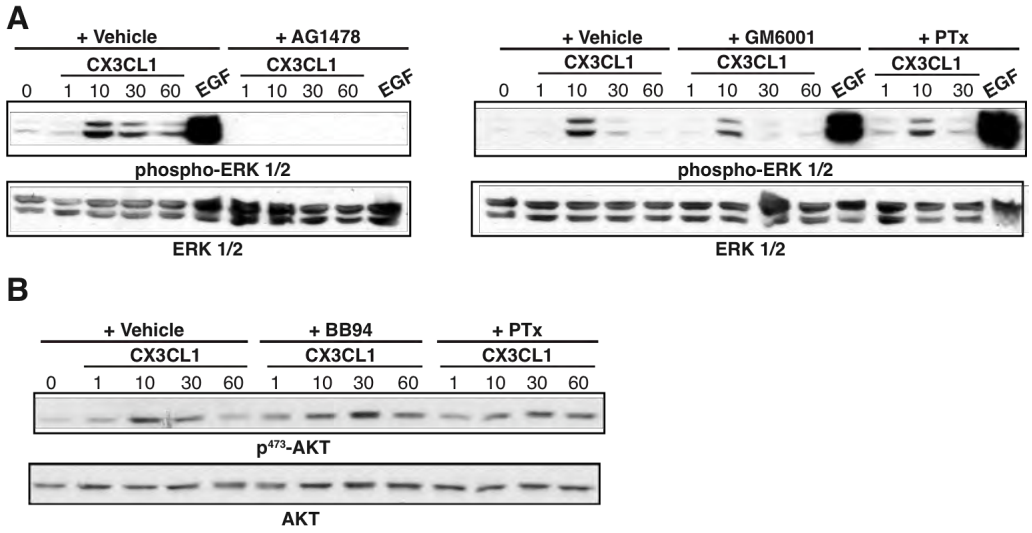

Supplementary Fig. S9. ***CX3CL1 induces transactivation of the EGF pathway.*** Analysis of CX3CL1-induced ERK (*A*) and AKT (*B*) activation in T47D cells. T47D cells were pretreated with inhibitors and stimulated with CX3CL1 for indicated times, or with EGF (10 min). Phosphorylated ERK 1/2 and AKT, and total ERK and AKT were determined in cell extracts. Representative blots from 4 independent experiments.

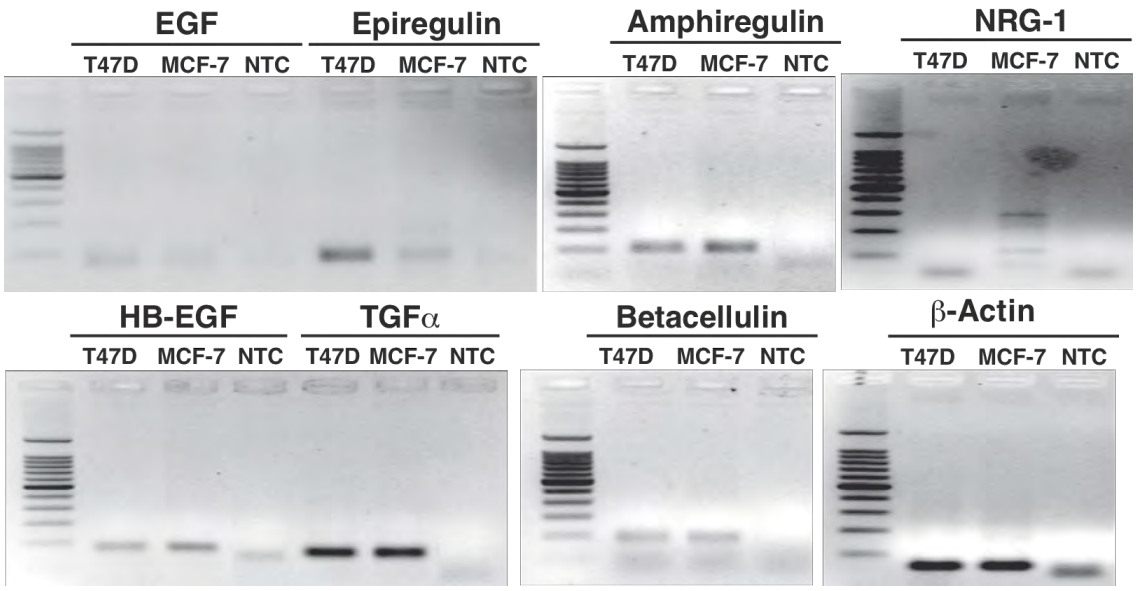

Supplementary Fig. S10. ***ErbB ligand expression in T47D cells.*** Total RNA of T47D cells or MCF-7 cells was retrotranscribed and assayed for PCR using the oligonucleotides and annealing temperatures indicated in Suppl. Table S2. Gels representative of two independent experiments. NTC; Non Template Control.

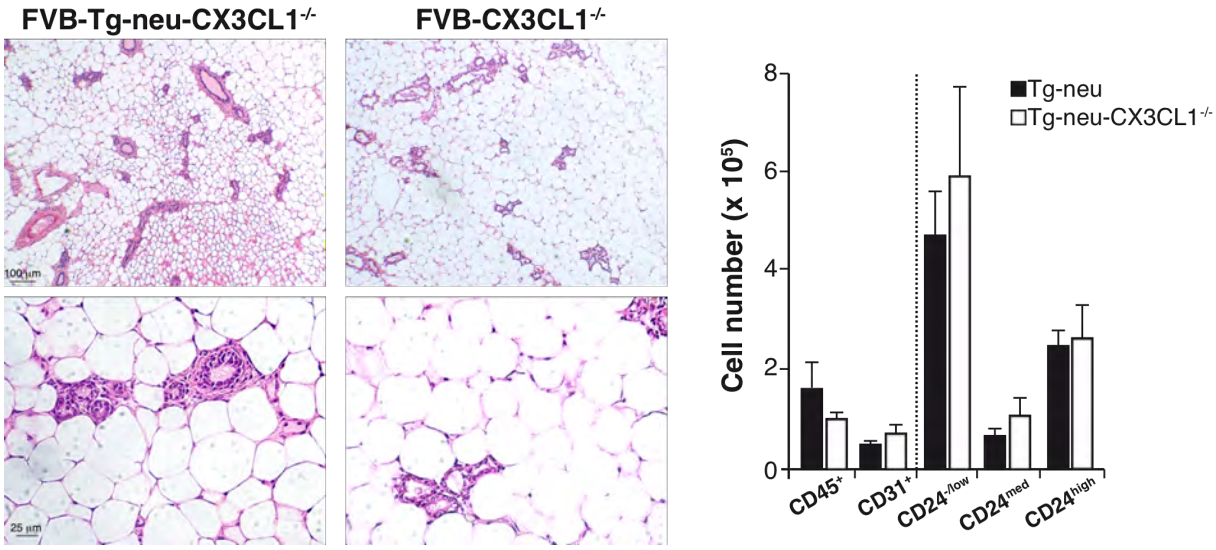

Supplementary Fig. S11. ***CX3CL1 deficiency does not affect the structure and composition of the mammary gland in Tg-neu mice.*** A, Representative hematoxylin/eosine stained sections of mammary glands from 8 to 12-weeks old nulliparous Tg-neu-CX3CL1$^{-/-}$ mice. B, Glands of Tg-neu and Tg-neu-CX3CL1$^{-/-}$ mice were digested, stained with antibodies against surface markers and analyzed by flow cytometry. Data are mean ± SEM of the total numbers for each cell subpopulation (n = 5, WT mice; n = 4 Tg-neu-CX3CL1$^{-/-}$ mice).

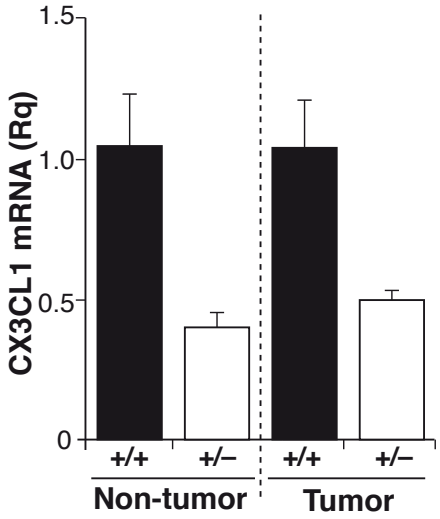

Supplementary Fig. S12. ***Hemizygous CX3CL1 mRNA expression in Tg-neu-CX3CL1$^{+/-}$ mice.*** CX3CL1 mRNA expression in healthy breast tissue (left) and breast carcinomas (right) derived from Tg-neu-CX3CL1$^{+/-}$ mice. Values were normalized to CX3CL1 mRNA levels expressed in Tg-neu mice for each condition (n = 4 mice/group).

Supplementary Table S1. ***Media used to culture the cancer cell lines***

Cell Line	Culture medium
N202.1A	DMEM plus 10% FCS, 1 mM sodium pyruvate, 1% non-essential amino acids
1G11	DMEM plus 20% FCS, 1 mM sodium pyruvate, 1% non-essential amino acids
MCF-10A	DMEM:F12 (1:1) plus 5% horse serum, hydrocortisone (0.5 μg/ml), EGF (20 ng/ml), insulin (10 μg/ml)
MCF-7	MEM plus 10% FCS, 1 mM sodium pyruvate, 1% non-essential amino acids
BT-474	RPMI 1640 plus 10% FCS, sodium bicarbonate (1.5 g/l), 1.2 mM oxalacetic acid, insulin (20 μg/ml)
T47D	RPMI 1640 plus 10% FCS, sodium bicarbonate (1.5 g/l)
MDA-MB-468	Leibovitz's L-15 plus 10% FCS
MDA-MB-231	DMEM plus 10% FCS
Hs578T	DMEM plus 10% FCS

Supplementary Table S2. ***Primers and annealing conditions used for PCR***

Gene[1]	Primers (Forward/Reverse)	Annealing (ºC, min)
(m) *b-actin*	5'- GGCACCACACCTTCTACAATG -3' 5'- TGGATGGCTACGTACATGGCTG -3'	67ºC, 1.5
(h) *b-actin*	5'- CCCAGCACAATGAAGATCAA 5'- CGATCCACACGGAGTACTTG	60ºC, 1.0
(m) *cx3cl1*	5'- CCGCGTTCTTCCATTTGTGT -3' 5'- AAGCCACTGGGATTCGTGAG-3'	67ºC, 1.5
(m) *cx3cr1*	5'- TGGCACTTCCTGCAGAAGTTC -3' 5'- GGCCTCAGCAGAATCGTCATA -3'	67ºC, 1.5
(h) *cx3cl1*	5'- CGGCAAACGCGCAATCATC -3' 5'- TTCTCGAAGGTGCCGCCATTT -3'	60ºC, 1.0
(h) *cx3cr1*	5'- TGACTGGCAGATCCAGAGGTT -3' 5'- GTTTTCTGTCACTGATTCAGGGAA -3'	60ºC, 1.0
(h) *snai1*	5'- CACTATGCCGCGCTCTTTC -3' 5'- GGTCGTAGGGCTGCTGGAA -3'	68ºC, 0.83
(h) *snai2*	5'- GGCAAGGCGTTTTCCAGAC -3' 5'- GCTCTGTTGCAGTGAGGGC -3'	59ºC, 0.83
(h) *twist1*	5'- CATGTCCGCGTCCCACTAG -3' 5'- TGTCCATTTTCTCCTTCTCTGG -3'	59ºC, 0.83
(h) *cdh1*	5'- AGAACGCATTGCCACATACACTC-3' 5'- CATTCTGATCGGTTACCGTGATC -3'	60ºC, 0.83
(h) *egf*	5'- AAGAATGGGGGTCAACCAGT -3' 5'- TGAAGTTGGTTGCATTGACC -3'	66ºC, 1.0
(h) *areg*	5'- TTTCAAAATTTCTGCATTCACG -3' 5'- ACTTTTCCCCACACCGTTC -3'	60ºC, 1.0
(h) *ereg*	5'- AGGATGGAGATGCTCTGTGC -3' 5'- TGAGGACTGCCTGTAGAAGATG -3'	66ºC, 1.0
(h) *hbegf*	5'- TGGGGCTTCTCATGTTTAGG -3' 5'- CATGCCCAACTTCACTTTCTC -3'	60ºC, 1.0
(h) *tgfa*	5'- GCTGCCACTCAGAAACAGTG -3' 5'- ATCTGCCACAGTCCACCTG -3'	60ºC, 1.0
(h) *btc*	5'- ACTGCATCAAAGGGAGATGC -3' 5'- TCTCACACCTTGCTCCAATG -3'	60ºC, 1.0
(h) *nrg-1*	5'- TGGTTCAAGAATGGGAATGA -3' 5'- CATCACTGGCTGATTCTGGA -3'	60ºC, 1.0

[1](h), human; (m), mouse; cdh1, e-cadherin; areg, amphiregulin; ereg, epiregulin; btc, betacellulin; nrg, neuregulin